FREQUENCY ISLANDS IN THE PRIMARY RESONANCE OF NONLINEAR DELAY SYSTEMS

Mohammed F. Daqaq
Assistant Professor
Mechanical Engineering Department
Clemson University
USA
mdaqaq@clemson.edu

Gregory W. Vogl
Postdoctoral Fellow
Manufacturing Engineering Laboratory
National Institute of Standards
USA
gvogl@nist.gov

Abstract

The purpose of this effort is to investigate primary resonances of nonlinear delay systems. Along these lines, the response of a Duffing oscillator with delayed-state feedback to primary resonance excitations is considered and analyzed using the method of multiple scales. Unlike previous research efforts that let the coefficients of the delay states (gains) be small to allow direct implementation of the method of multiple scales, we demonstrate that the method can be adapted to analyze nonlinear delay systems with large gains. Further, we unveil very interesting dynamic responses characterized by the presence of *islands* in the frequency response of the delayed Duffing oscillator. It is demonstrated that these islands grow in size and collide with the main branch of solutions (*mainland*) as the magnitude of the external excitation is increased or as the gain-delay combination is chosen closer to the stability boundaries of the free response.

Key words

Primary Resonance, Delay Systems, Frequency Islands.

1 Introduction

1.1 Overview

Time-delay, *hereditary*, *retarded*, or *time-lag* represent different descriptions of dynamic systems that do not react instantaneously to actuation signals or whose temporal evolution is based on retarded communications or information from the past. The first systematic work on delay systems started in the early 1900s with the epidemiological studies on the prevention of malaria by Ross [Ross, 1911] followed by the work of Lotka [Lotka, 1923] in 1923, who indicated the necessity of including time-delays to account for the malaria incubation times in Ross' model. In 1927, Volterra [Volterra, 1927] introduced the retarded forms of predator-prey models used to describe population dynamics, while Minorski, in 1942, was among the first to address the presence of delays in mechanical systems [Minorski, 1942].

Subsequently, there has been a substantial increase of research activities directed towards understanding the effects of time delays on the stability of various dynamic systems. This established a flourishing new branch of mathematics primarily concerned with stability and stabilization of Delay-Differential Equations (DDEs). Along these lines, a variety of analytical, graphical, and numerical methodologies have been proposed and implemented to capture and assess the stability of systems operating with single, multiple, discrete, or continuous time delays.

1.2 Background and Motivation

Despite the significant body of research that deals with the stability and stabilization of delay systems, most of the previous efforts were directed towards characterizing the stability of the free response by proposing various methodologies to predict and estimate the location of the eigenvalues relative to the imaginary axis [Diekmann, 1995; Bellman and Cooke, 1963]. Little attention has been paid to understanding the effect of time delays on the response of nonlinear *externally-excited systems* [Hu, 1998 ; Ji and Leung, 2002]. In particular, the nonlinear response of a delayed system to primary-resonance excitations has yet to be addressed comprehensively. Such studies were not necessary in the past due to the limited number of applications in which time delays and external excitations coexist in the operation of a dynamic system.

However, due to the emergence of micro and nanodevices as the next generation sensors and actuators, this type of analysis is becoming more imperative. Microdevices are usually excited at one of their resonant frequencies with feedback control algorithms implemented to close the loop and provide real-time information about the states [Garcia and Perez, 2002]. Due to their large natural frequencies, these devices have relatively small response periods. The very small measurement delays in the control loop can then be of the same order as the response period, thereby channeling energy into or out of the system at incorrect time intervals and producing instabilities that render traditional controllers' performance ineffective [Stark, 2005].

To resolve these issues, there is a growing interest in the controls and dynamics communities to utilize delayed-feedback controllers for vibration mitigation and control of microsystems. It has been shown that augmenting the system delay with a carefully and deliberately selected delay period is capable of producing substantial damping that can actually aid controller design [Abdallah, 1993]. As a result, delayed-feedback algorithms have been successfully implemented to control microcantilevers in dynamic force microscopy [Yamasue and Hikihara, 2006], to eliminate chaotic motions in tapping-mode atomic force microscopy [Sadeghian, 2007], for sensor sensitivity enhancement in nanomechanical cantilever sensors [Daqaq, 2007; Bradely, 2007], and to control the quality factor in dynamic atomic force microscopy [Stark, 2005].

Successful implementation of these controllers to nonlinear delay systems requires a deep analytical understanding of the primary resonance phenomenon in time-delayed systems, especially when the objective is to control an externally-excited system. Hu et al. [Hu, 1998] studied the primary resonance of a Duffing oscillator subjected to both position and velocity delayed-feedback control. Similarly, Ji and Leung [Ji and Leung, 2002] and Jin and Hu [Jin and Hu, 2007] studied the primary resonance of a Duffing oscillator with two time delays in the state feedback. However, all of these studies were restricted to systems with linear delay terms that have very small coefficients (*gains*). Accordingly, the method of multiple scales [Nayfeh, 1981] was directly implemented to obtain uniform analytical approximate solutions because the gains could be scaled at the highest order of the perturbation problem with the nonlinearities, internal damping, and external excitation. For many applications, however, especially feedback control, these coefficients can be relatively large. By scaling the linear gains at the highest order of the perturbation problem, one implicitly assumes that the response of the delay system can be approximated by the first-delay frequency which, in general, is very close to the system's natural frequency. When the gains are large, sticking to this assumption could produce erroneous qualitative and quantitative predictions that would hide some of the essential features of the nonlinear response [Daqaq and Alhazza].

1.3 Problem Statement

In this work, we propose a modification to the approach presented earlier in Refs. [Hu, 1998] and [Ji and Leung, 2002]. Again, we make use of the method of multiple scales but adapt the implementation procedure to allow for the alleviation of the small gain restriction. Utilizing the resulting solution, we uncover interesting dynamic responses. These responses are characterized by the presence of *frequency islands* that have critical implications on the global stability of the response. Such islands could yield undesired consequences, especially when delayed-feedback algorithms are applied to mitigate oscillations of externally-excited systems.

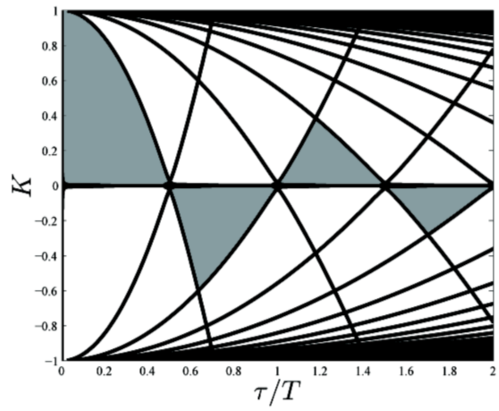

Figure 1. Stability map of the equilibrium solutions of Equation (1) for $j = 2$. Shaded regions represent asymptotically stable equilibria. Results are obtained for $\omega_n = 1$, $\mu = 0.005$, and $T = 2\pi/\omega_n$.

2 Linear Analysis

2.1 Free Response:

Consider the Duffing oscillator with delayed-state feedback

$$\frac{d^2u}{dt^2} + 2\mu\frac{du}{dt} + \omega_n^2 u = -K\frac{d^j u(t-\tau)}{dt^j} - \alpha u^3 + F\cos(\Omega t) \qquad j = 0,1,2 \tag{1}$$

where $u \in \mathcal{R}$ is the state, $\mu \in \mathcal{R}^+$ is a linear damping term, $\omega_n \in \mathcal{R}^+$ is the natural frequency, $K \in \mathcal{R}$ is the coefficient of the linear-delayed state, loosely referred to as the gain, $\tau \in \mathcal{R}^+$ is a discrete time delay, $\alpha \in \mathcal{R}$ is the coefficient of cubic nonlinearity and j is the order of the delayed-state derivative. We note that the Einstein convention does not apply.

The local stability of the equilibrium solutions of the unforced system can be determined by finding the eigenvalues, λ, of the linearized equation when F equals zero. These eigenvalues are obtained by substituting a homogeneous solution of the form, $u_h = c\,exp(\lambda t)$, into Equation (1) to yield

$$(\omega_n^2+\lambda^2)+2\mu\lambda+K\lambda^j e^{-\lambda\tau} = 0, \qquad j = 0,1,2. \tag{2}$$

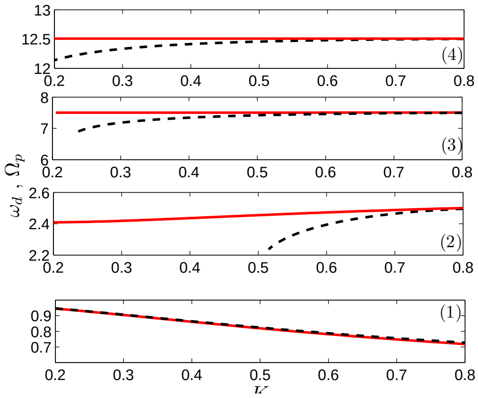

Figure 2. Variation of the first four delay frequencies, ω_d, (solid lines) and the associated peak frequencies, Ω_p, (dashed lines) with the gain K. Results are obtained for a fixed delay $\tau = 0.2\pi$, $\omega_n = 1$, $\mu = 0.005$ and $j = 2$

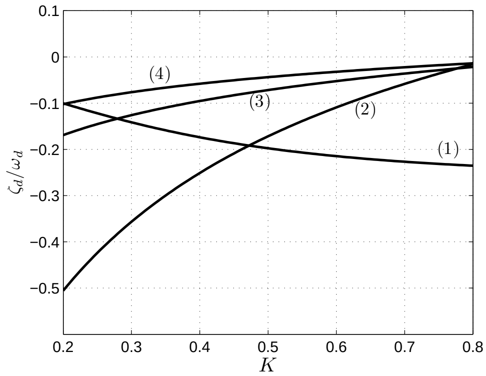

Figure 3. Variation of the associated damping ratios ζ_d/ω_d with the gain K. Results are obtained for a fixed delay $\tau = 0.2\pi$, $\omega_n = 1$, $\mu = 0.005$ and $j = 2$

Equation (2) is a transcendental characteristic equation that has an infinite number of solutions associated with every set of fixed parameters (K,τ). By inspecting the form of the homogeneous solution, u_h, it becomes evident that the stability of the equilibrium solutions is determined by the sign of the real part of the eigenvalues ($\lambda = \zeta_d \pm i\omega_d$). In particular, the equilibrium solutions are locally asymptotically stable if all the eigenvalues have negative real parts, $\zeta_d < 0$, and unstable if at least one eigenvalue has a positive real part, $\zeta_d > 0$. Thus, to determine the stability boundaries, we set the real part of the eigenvalue ζ_d equal to zero and substitute $\lambda = i\omega_d$ into Equation (2), then separate the real and imaginary parts of the outcome to obtain

$$(\omega_n^2 - \hat{\omega}_d^2) + (-1)^j \hat{K} \frac{\partial^j}{\partial \hat{\tau}^j} \left\{ \cos(\hat{\omega}_d \hat{\tau}) \right\} = 0, \tag{3a}$$

$$2\mu\hat{\omega}_d - (-1)^j \hat{K} \frac{\partial^j}{\partial \hat{\tau}^j} \left\{ \sin(\hat{\omega}_d \hat{\tau}) \right\} = 0, \qquad j = 0, 1, 2. \tag{3b}$$

where the hat denotes a value at the stability boundary. For a given gain $\hat{K}$, Equations (3) can be solved for the delay $\hat{\tau}$ and the associated frequency at the boundary, $\hat{\omega}_d$. To better visualize the stability of the equilibrium solutions, the gain-delay space is mapped into stable and unstable regions as depicted in Fig. 1, where shaded regions represent gain-delay combinations leading to asymptotically stable equilibria.

2.2 Forced Response:

2.2.1 The Steady-State Solution In the remainder of this work, we limit the analysis to gain-delay combinations leading to stable equilibrium solutions. In other words, we only consider gain-delay values in the shaded regions depicted in Fig. 1. As such, the homogeneous linear solution of Equation (1), u_h, decays with time and does not affect the steady-state response. Next, to determine the steady-state linear response of the forced system, we retain the linear terms in Equation (1) and assume a solution of the form

$$u_{ss}(t) = \frac{1}{2} a e^{i(\Omega t + \gamma)} + cc \tag{4}$$

where a and γ are, respectively, the steady-state amplitude and phase of the response and cc is the complex conjugate of the preceding term. We substitute Equation (4) into the linearized version of Equation (1), set the real and imaginary parts of the resulting expression equal to zero, and obtain

$$\left((\omega_n^2 - \Omega^2) + (-1)^j K \frac{\partial^j}{\partial \tau^j} [\cos(\Omega\tau)] \right) a = -F \cos\gamma \tag{5a}$$

$$\left(2\mu\Omega - (-1)^j K \frac{\partial^j}{\partial \tau^j} [\sin(\Omega\tau)] \right) a = F \sin\gamma, \qquad j = 0, 1, 2 \tag{5b}$$

The linear steady-state amplitude of the response can be obtained by squaring and adding Equations (5) then solving the resulting equation for a. The corresponding phase, γ, is obtained by using either one of Equations (5). Accordingly, the steady-state response can be written as

$$u_{ss}(t) = a\cos(\Omega t + \gamma) \tag{6}$$

where

$$a = F \Bigg/ \left\{ \left(\omega_n^2 - \Omega^2 + (-1)^j K \frac{\partial^j}{\partial \tau^j} [\cos(\Omega\tau)] \right)^2 + \left(2\mu\Omega - (-1)^j K \frac{\partial^j}{\partial \tau^j} [\sin(\Omega\tau)] \right)^2 \right\} \quad \text{(7a)}$$

$$\gamma = -\arctan \frac{2\mu\Omega - (-1)^j K \frac{\partial^j}{\partial \tau^j} [\sin(\Omega\tau)]}{\omega_n^2 - \Omega^2 + (-1)^j K \frac{\partial^j}{\partial \tau^j} [\cos(\Omega\tau)]} \quad \text{(7b)}$$

2.2.2 Peak Versus Delay Frequencies

Similar to continuous systems, delay systems could exhibit peak responses (resonances) at a large number of frequencies. The peaks can be determined by minimizing the denominator of Equation (7a) with respect to the excitation frequency. The minimization problem requires that the first derivative of the denominator with respect to Ω vanishes and that the second derivative is greater than zero. It turns out that these equations do not always yield a unique solution. As such, the frequency-response curves of the forced response may exhibit more than one peak. To further illustrate this fact, we consider the assumption of small internal damping, gain, and delay. In other words, we let $\mu = \epsilon\mu$, $K = \epsilon K$, and $\tau = \epsilon\tau$, undertake the minimization problem, then eliminate terms having higher orders of ϵ to obtain

$$\cos\left(\frac{\pi j}{2} + \tau\Omega_p\right) = \frac{2(-1)^{-j}\Omega_p^{2-j}\left(\Omega_p^2 - \omega_n^2\right)}{K\left(j(\Omega_p^2 - \omega_n^2) + 2\Omega_p^2\right)}, \quad j = 0, 1, 2. \quad \text{(8)}$$

or

$$\cos\left(\frac{\pi j}{2} + \tau\Omega_p\right) - O\left(\frac{\Omega_p^{2-j}}{K}\right) = 0 \qquad j = 0, 1, 2. \quad \text{(9)}$$

where Ω_p is the peak frequency and O denotes "*the order of*". By examining Equation (9), it becomes evident that the number of peak frequencies is directly proportional to both j and the magnitude of K. Hence, a delay system can exhibit more than one peak frequency. For instance, at $\tau = 1.2\pi$, $K = -0.4$, $j = 2$, $\omega_n = 1$, and $\mu = 0.005$ the frequency-response exhibits a very large number of peak frequencies, out of which, the lowest three are listed herein: $\Omega_{p1} = 0.841806$, $\Omega_{p2} = 1.61982$, $\Omega_{p3} = 3.29911$.

The preceding discussion is aimed at demonstrating that delay systems can exhibit primary resonances at a large number of frequencies. Depending on the gain and delay values, these resonances may occur at frequencies that are far from the natural frequency ω_n. Further, not every delay frequency, ω_d, obtained via the linear unforced eigenvalue problem yields a peak frequency. This can be understood by noting that, associated with every nonzero set of parameters (K, τ), the free response always yields an infinite number of eigenfrequencies, ω_d. On the other hand, as illustrated in Equation (9), the number of peak frequencies depends on the values of j and K.

To further illustrate the relation between the peak frequencies, Ω_p, and the imaginary parts of the eigenvalues, ω_d, Fig. 2 displays variation of the first four peak and delay frequencies with the gain for $j = 2$ and a fixed delay, $\tau = 0.2\pi$. The figure shows that the first delay frequency, ω_{d1}, coincides with the the first peak frequency, Ω_{p1}, over the whole gain range. The second peak frequency, ω_{p2}, however exists only for values of K greater than $K \approx 0.5$ and approaches the second-delay frequency, ω_{d2}, only when the gain is large. The convergence between these frequencies at large gains can be attributed to a decrease in the absolute value of the damping parameter, ζ_{d2}, associated with the second-delay frequency as depicted in Fig. 3. The third and fourth peak frequencies exist for smaller gains but only converge to the delay frequencies as the gain is increased.

2.3 Implementation of the Method of Multiple Scales

It has been shown in the previous section that delay systems exhibit a large number of peak frequencies and that these frequencies are not necessarily close to ω_n. Further, one would expect that, similar to continuous systems, the nonlinear response in the vicinity of each frequency could have a qualitatively different behavior. As such, the response of a delay system can not be captured by simply assuming that the response can be approximated by one frequency that is very close to the system's natural frequency unless the gains are very small [Hu, 1998]. In this section, we propose a methodology to alleviate this assumption. Towards that end, we extract the delay from the linear states and write Equation (1) in the following form:

$$\frac{d^2u}{dt^2} + 2|f_1(K,\tau)|\frac{du}{dt} + |f_2(K,\tau)|u = F\cos(\Omega t) - \alpha u^3 \quad \text{(10)}$$

where f_1 and f_2 are unknown nonzero functions that will be determined at a later stage in the perturbation analysis. As mentioned earlier, since the analysis is limited to asymptotically stable free responses, absolute values of the unknown functions are used to ensure this condition.

Using the method of multiple scales, we seek a second-order nonlinear solution in the form

$$u(T_0, T_1) = u_0(T_0, T_1) + \epsilon u_1(T_0, T_1) + O(\epsilon^2) \quad \text{(11)}$$

where $T_n = \epsilon^n t$ and ϵ is a small bookkeeping parameter. In terms of the T_n, the time derivative becomes

$$\frac{d}{dt} = D_0 + \epsilon D_1 + O(\epsilon^2) \tag{12}$$

where $D_n = \partial/\partial T_n$. To analyze the effect of the primary resonance excitation, the amplitude of excitation and nonlinearities are ordered so that they appear in the same perturbation equation as f_1. In other words, we let

$$f_1 = \epsilon f_1, \qquad F = \epsilon F, \qquad \alpha = \epsilon \alpha, \qquad \beta = \epsilon \beta \tag{13}$$

We express the nearness of the excitation frequency, Ω, to the unknown function, f_2, by introducing a detuning parameter, σ, and letting

$$\Omega^2 = |f_2| + \epsilon \sigma \tag{14}$$

For small ϵ, Equation (14) can be written as

$$\Omega \approx \sqrt{|f_2|} + \frac{1}{2\sqrt{|f_2|}} \epsilon \sigma \tag{15}$$

Substituting Equation (11), (13), and (15) into Equation (10) and equating coefficients of like powers of ϵ, we obtain

$$O(1): \quad D_0^2 u_0 + |f_2| u_0 = 0 \tag{16}$$

$$\begin{aligned} O(\epsilon): \quad & D_0^2 u_1 + |f_2| u_1 = -2 D_0 D_1 u_0 - 2|f_1| D_0 u_0 \\ & + F \cos(\sqrt{|f_2|} T_0 + \sigma \sqrt{|f_2^{-1}|} T_1) \\ & - \alpha u_0^3 \end{aligned} \tag{17}$$

The solution of the first order equation, Equation (16), can be written as

$$u_0 = A(T_1) e^{i\sqrt{|f_2|} T_0} + \bar{A}(T_1) e^{-i\sqrt{|f_2|} T_0} \tag{18}$$

Substituting Equation (18) into Equation (17) and eliminating the terms that produce secular terms in the solution yields

$$\begin{aligned} -2i\sqrt{|f_2|} D_1 A - 2i|f_1|\sqrt{|f_2|} A + \frac{F}{2} e^{i\sigma\sqrt{|f_2^{-1}|} T_1} \\ - 3\alpha A^2 \bar{A} = 0 \end{aligned} \tag{19}$$

To construct the modulation equations, we introduce the polar transformation $A(T_1) = a(T_1) e^{i\beta(T_1)}/2$ and substitute it into Equation (19), then separate the real and imaginary parts of the outcome to obtain

$$\sqrt{|f_2|} a\prime = -(|f_1|\sqrt{|f_2|}) a + \frac{F}{2} \sin\gamma \tag{20a}$$

$$\sqrt{|f_2|} a\gamma\prime = \frac{(\Omega^2 - |f_2|)}{2} a - \frac{3\alpha}{8} a^3 + \frac{F}{2} \cos\gamma \tag{20b}$$

where the prime denotes differentiation with respect to T_1, $\gamma = \sigma\sqrt{|f_2^{-1}|} T_1 + \beta$. Now, substituting $T_1 = \epsilon t$ into Equations (20), then setting the bookkeeping parameter ϵ equal to 1 yields

$$\sqrt{|f_2|} \dot{a} = -(|f_1|\sqrt{|f_2|}) a + \frac{F}{2} \sin\gamma \tag{21a}$$

$$\sqrt{|f_2|} a\dot{\gamma} = \frac{(\Omega^2 - |f_2|)}{2} a - \frac{3\alpha}{8} a^3 + \frac{F}{2} \cos\gamma \tag{21b}$$

where the dot denotes differentiation with respect to time, t. For the steady-state response, $\dot{a} = \dot{\gamma} = 0$. It follows from Equations (21a) and (21b) that

$$f_1^2 |f_2| a_0^2 + \left(\frac{(|f_2| - \Omega^2)}{2} a_0 - \frac{3\alpha}{8} a_0^3 \right)^2 = \frac{F^2}{4} \tag{22}$$

and

$$\tan\gamma_0 = \frac{|f_1|\sqrt{|f_2|} a_0}{\frac{(|f_2| - \Omega^2)}{2} a_0 - \frac{3\alpha}{8} a_0^3} \tag{23}$$

where a_0 and γ_0 are, respectively, the steady-state amplitude and phase of the response. Setting α equal to zero in Equations (22) and (23), one would expect to obtain the linear steady-state amplitude and phase of the response as given by Equations (7). Therefore, f_1 and f_2 are determined by enforcing the linear steady-state amplitude and phase obtained via Equations (22) and (23) to equal those acquired via Equations (6) and (7). Imposing these conditions, we obtain

$$\begin{aligned} f_2 &= \omega_n^2 + (-1)^j K \frac{\partial^j}{\partial \tau^j} [\cos(\Omega\tau)] \\ f_1 &= \frac{1}{2\sqrt{|f_2|}} (2\mu\Omega - (-1)^j K \frac{\partial^j}{\partial \tau^j} [\sin(\Omega\tau)]) \\ & j = 0, 1, 2. \end{aligned} \tag{24}$$

As one would expect, for small values of K and σ, f_2^2 approaches ω_n and f_1 approaches μ. To assess the stability of the resulting solutions, we find the eigenvalues of the Jacobian of the modulation equations evaluated at the roots (a_0, γ_0) and characterize the sign of their real parts.

In Fig. 4, we validate the modified perturbation solution by comparing the frequency-response curves to solutions acquired via the method of harmonic balance. By inspecting Fig. 4, it is evident that the modified approach yields results that are almost indistinguishable

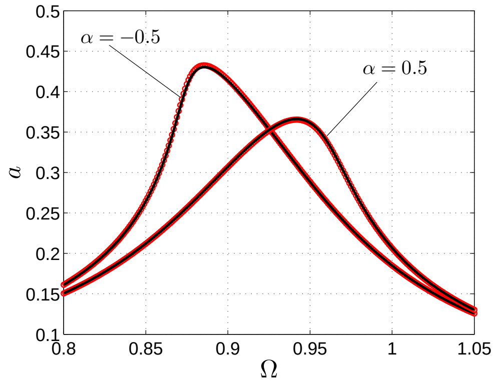

Figure 4. Nonlinear frequency-response curves obtained using the method of harmonic balance (circles) and the method of multiple scales (solid lines). Results are obtained for $K = 0.2, \tau = 0.2\pi, j = 2$, and $F = 0.04$.

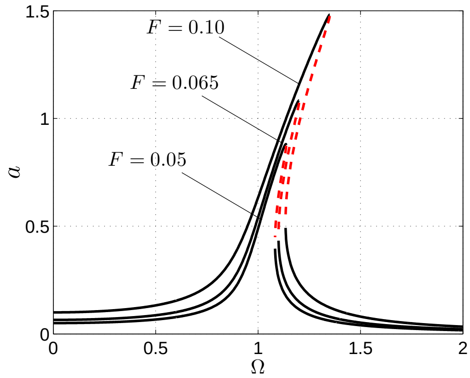

Figure 5. Frequency-response curves for different excitation magnitudes and zero gain ($K = 0$). The other parameters used are $j = 2$, $\tau = 0.7\pi$, $\alpha = 0.5$, $\omega_n = 1$, and $\mu = 0.005$.

from those obtained using the harmonic balance (*solutions are on top of each other*). It is also evident that the methodology closely predicts the frequency-response curves even for large values of K and is capable of capturing the effect of different nonlinear coefficients on the response.

2.4 Frequency Island Behavior

For small forcing magnitudes, the feedback controller may reduce the response amplitude significantly. The frequency-response curves before application of a delayed feedback are shown in Fig. 5 and illustrate large-response amplitudes, hardening-type behavior, and hysteretic jumps. Clearly, there is at least one stable branch of steady-state solutions associated with every excitation frequency. In order to decrease this stable response amplitude, a gain, $K = 0.4$, and an associated delay, $\tau = 0.7\pi$, are chosen as parameters for the feedback controller. The frequency-response curves for various forcing magnitudes are seen in Fig. 6. For the case with the relatively small forcing magnitude, $F = 0.05$, the feedback has caused the undelayed peak amplitude to decrease from about 0.8 in Fig. 5 to approximately 0.3 in Fig. 6, which is a decrease of more than 50 percent.

Along with the stable solution branch, *mainland*, there exists unstable *islands* in the frequency-response curves in Fig. 6. Frequency island generation was encountered previously by very few researchers including Narimani et al. [Narimani, 2002] in their analysis of a piecewise linear system under harmonic excitation, and by Lacarbonara et al. [Lacarbonara, 2005] in studying the nonlinear modal interactions of imperfect beams at veering. In both cases, the frequency islands are created by either two stable branches of solutions or at least contained one stable branch of dynamic solutions. On the other hand, the frequency islands here are formed by two *unstable* solution branches.

As the forcing is increased, the island increases in size

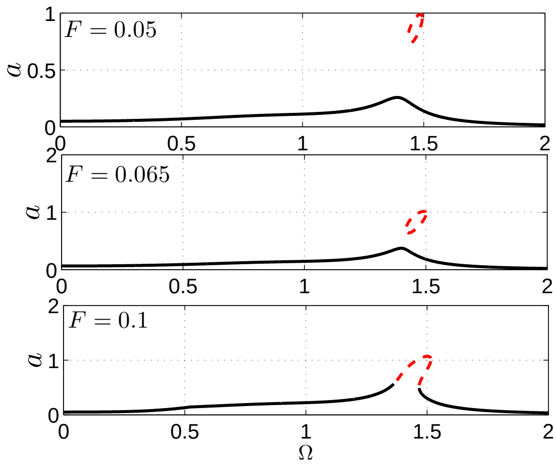

Figure 6. Frequency-response behavior and frequency islands for increasing forcing amplitudes. Dashed lines represent unstable solutions. Results are obtained for $j = 2$, $\tau = 0.7\pi$, $K = 0.4$, $\alpha = 0.5$, $\omega_n = 1$, and $\mu = 0.005$.

and grows closer to the mainland until they collide at a critical forcing amplitude, as illustrated in the descending subfigures within Fig. 6. Initial investigation also reveals that these frequency islands grow in size and collide with the mainland as the delay is chosen closer to the stability boundary. For instance, Figure 7 reveals mainland destruction as the delay time increases.

Consequently, there will be a region of excitation frequencies for which no stable solution exists. For example, as shown in Fig. 8, the response amplitude grows without limits when the system is excited at a frequency that falls within the new region without a mainland. This result has critical implications on implementing delayed-feedback controllers to stabilize externally-excited nonlinear systems, since *for some gain-delay combinations that yield a linearly-stable free response, the nonlinear forced response could grow without bounds.*

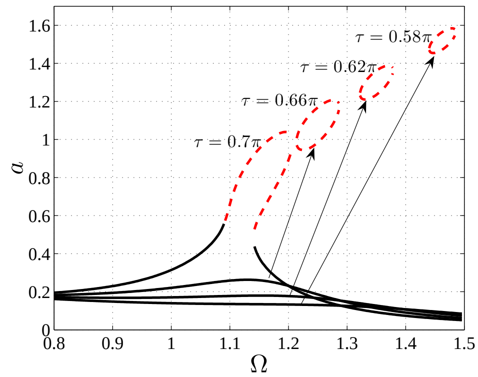

Figure 7. Frequency-response behavior and frequency islands for increasing delays (getting closer to the stability boundary of the free response). Dashed lines represent unstable solutions. Results are obtained for $j = 2$, $K = 0.4$, $\alpha = 0.5$, $\omega_n = 1$, $F = 0.05$, and $\mu = 0.005$.

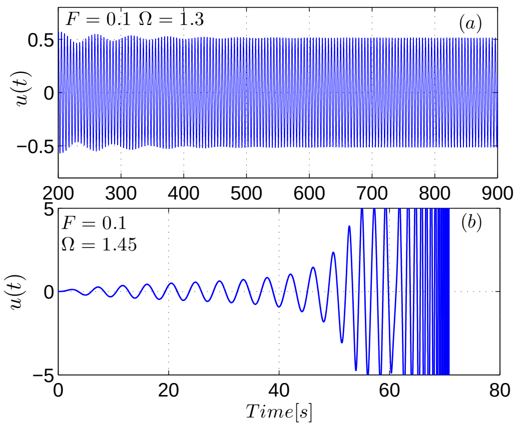

Figure 8. Time histories of the response at (a) $\Omega = 1.3$ and (b) $\Omega = 1.45$. Results are obtained for $j = 2$, $\tau = 0.35\pi$, $K = 0.4$, $\alpha = 0.5$, $\omega_n = 1$, $F = 0.05$, and $\mu = 0.005$.

References

Abdallah, C., P. Dorato, Benitez-Read and R. Byrne (1993). Delayed-Positive Feedback Can Stabilize Oscillatory Systems. In: *Proceedings of the 1993 American Control Conference*. pp. 3106–3107.

Bellman, R. E. and K. L. Cooke (1963). *Differential Difference Equations*. Academic Press. New York.

Bradely, C., M.F. Daqaq and N. Jalili (2007). Experimental Study on Utilizing Delayed Feedback for Ultra-Sensitive Sensing. In: *Proceedings of the IMECE 2007, International Mechanical Engineering Conference and Exposition*. Seattle, WA.

Daqaq, M. F. and K. A. Alhazza (Under Review). On The Primary Resonances of Nonlinear Delay Systems. *ASME Journal of Computational and Nonlinear Dynamics*.

Daqaq, M.F., C. Bradely and N. Jalili (2007). Feedback Delays for Ultrasensitive Sensing. In: *Proceedings of the ASME 2007 International Design and Engineering Technical Conference And Computers and Information in Engineering Conference*. Las Vegas, NV.

Diekmann, O., S. A. Van Gils, S. M. Verduyn-Lunel and H. O. Walther (1995). *Delay Equations, Functional, Complex and Nonlinear Analysis Difference Equations*. Springer-Verlag. New York.

García, R. and R. Pérez (2002). Dynamic atomic force microscopy methods. *Surface Science Reports* **47**, 197–301.

Hu, H., E. Dowell and L. Virgin (1998). Resonance of a Harmonically Forced Duffing Oscillator with Time Delay State Feedback. *Nonlinear Dynamics* **15**, 311.

Ji, J. C. and A. Y. T. Leung (2002). Resonances of a Nonlinear SDOF System with Two Time-Delays in Linear Feedback Control. *Nonlinear Dynamics* **253**, 985.

Jin, Y. and H. Hu (2007). Primary Resonance of A Duffing Oscillator with Two Distinct Time Delays in State Feedback under Narrow-Band Random Excitation. In: *Proceedings of the ASME 2007 International Design and Engineering Technical Conference And Computers and Information in Engineering Conference*. Las Vegas, NV.

Lacarbonara, W. and H. N. Arafat and Nayfeh A. H. (2005). Nonlinear Interactions in Imperfect Beams at Veering. *International Journal of Nonlinear Mechanics* **40**, 987–1003.

Lotka, A. J. (1923). Contributions to The Analysis of Malaria Epidemiology:I General Part. *Supplement to American Journal of Hygiene* **3**, 1–37.

Minorski, N. (1942). Self-Excited Oscillations in Dynamical Systems Possessing Retarded Actions. *Journal of Applied Mechanics* **9**, 65–71.

Narimani, A. and J.G. Nakhaie and M.F. Golnaraghi (2002). Sensitivity Analysis of Frequency Response of A Piecewise Linear System in Frequency Island. In:*Proceedings of the Ninth Conference on Nonlinear Vibrations, Stability, and Dynamics of Structures*. Blacksburg, VA.

Nayfeh, A. H. (1981). *Introduction to Perturbation Techniques*. Wiley-Interscience. New York.

Ross, K. (1911). *The Prevention of Malaria*. Second Edition, London: John Murray.

Sadeghian, H., M. T. Arjmand, H. Salarieh and A. Alasty (2007). Chaos Control in Single Mode Approximation of T-AFM Systems Using Nonlinear Delayed Feedback Based on Sliding Mode Control. In: *Proceedings of the ASME 2007 International Design and Engineering Technical Conference And Computers and Information in Engineering Conference*. Las Vegas, NV.

Stark, R. W. (2005). Time Delay Q-Control of the Microcantilever in Dynamic Atomic Force Microscopy. In: *Proceedings of 2005 5th IEEE Conference on Nanotechnology*. Nagoya, Japan.

Volterra, V. (1927). Variazioni et Fluttuazioni del Numero D'individuali in Specie Animali Conviventi. *R. Comitato Talassografico Memoria* **131**, 1–142.

Yamasue, K. and T. Hikihara (2006). Control of Microcantilevers in Dynamic Force Microscopy Using Time-Delayed Feedback. *Review of Scientific Instruments* **77**, 1–6.